Application of tobacco hairy roots for the removal of malachite green from aqueous solutions: experimental design, kinetic, equilibrium, and thermodynamic studies.

Journal:	*Chemical Engineering Communications*
Manuscript ID	GCEC-2017-0281.R2
Manuscript Type:	Research Paper
Date Submitted by the Author:	n/a
Complete List of Authors:	Escudero, Leticia; Universidad Nacional de Cuyo, Facultad de Ciencias Exactas y Naturales, Laboratory of Analytical Chemistry for Research and Development (QUIANID) Agostini, Elizabeth; Universidad Nacional de Rio Cuarto, Departamento de Biología Molecular Dotto, Guilherme; Federal University of Santa Maria,
Keywords:	Hairy roots, Malachite Green, Biosorption, Dye removal, Kinetics, Thermodynamics

Application of tobacco hairy roots for the removal of malachite green from aqueous solutions: experimental design, kinetic, equilibrium, and thermodynamic studies

Running Head: Removal of malachite green using tobacco hairy roots

LETICIA B. ESCUDERO[1,2,*], ELIZABETH AGOSTINI[2,3], GUILHERME L. DOTTO[4]

[1]Laboratory of Analytical Chemistry for Research and Development (QUIANID), Facultad de Ciencias Exactas y Naturales, Universidad Nacional de Cuyo, Padre J. Contreras 1300, (5500) Mendoza, Argentina.

[2]Consejo Nacional de Investigaciones Científicas y Técnicas (CONICET), Argentina.

[3]Departamento de Biología Molecular, FCEFQyN, Universidad Nacional de Río Cuarto, Córdoba, Argentina.

[4]Chemical Engineering Department, Federal University of Santa Maria (UFSM), 1000 Roraima Avenue, 97105–900, Santa Maria, RS, Brazil.

*Corresponding author: Laboratory of Analytical Chemistry for Research and Development (QUIANID), Facultad de Ciencias Exactas y Naturales, Universidad Nacional de Cuyo, Padre J. Contreras 1300, (5500) Mendoza, Argentina.

E–mail address: letibelescudero@gmail.com

Abstract

Tobacco hairy roots (THR) were used to evaluate its potential for the biosorption and removal of malachite green (MG) from aqueous solutions. A 3^2 full factorial design was applied to study the effects of pH and THR concentration on the biosorption capacity. Under the optimal conditions (pH of 7.0 and THR concentration of 1g L^{-1}), dye removal efficiency was around 92%. Experimental data obtained from kinetic studies demonstrated good concordance with the pseudo−second order model. Equilibrium studies were developed and the data was evaluated by Langmuir, Freundlich, and Sips models, being the Sips model the most adequate (maximum biosorption capacity of 277.2 mg g^{-1}). Thermodynamically, the biosorption of MG on THR proved to be endothermic, spontaneous, and favorable. Desorption was feasible under acidic conditions and the biosorbent could be reused three times. THR was tested in simulated effluent and the removal percentage was 87%, demonstrating that this material is a promising biosorbent which can be used to treat colored wastewaters.

Keywords Hairy roots; Malachite Green; Biosorption; Dye removal; Kinetics; Thermodynamics.

Introduction

Malachite green (MG) is a triphenylmethane cationic dye widely used in textile industry. It is highly toxic and has proved to be effective against a wide variety of pathogen agents, including fungus, bacteria, and parasites (Zhang et al., 2008). Malachite green can cause severe effects in human health due to its carcinogenic, mutagenic, and teratogenic properties (Banerjee et al., 2016). Moreover, this organic molecule can affect aquatic life and provoke irreversible hurt in several organs, such as liver, kidney, and intestine. Although MG has been cataloged as a banned drug for aquaculture in many countries, the illegal use is still present, due to its low cost and high efficiency (Li et al., 2017). Therefore, studies focused on removal of MG from aqueous solutions are of great relevance, not only for preservation of public health but also for environmental protection.

Several treatments have been applied for the removal of MG from contaminated wastewaters, including biological treatment (Daneshvar et al., 2007), coagulation/flocculation (Man et al., 2012), electrochemical oxidation (Bañuelos et al., 2016; Sasidharan Pillai and Gupta, 2016), and adsorption/biosorption (Das et al., 2009; Jerold and Sivasubramanian, 2016). For years, biosorption concept has been understood as a promising clean−up biotechnology and researchers performed efforts to prepare new efficient, low cost, and environmental friendly materials for the removal of contaminants from wastewaters (Fomina and Gadd, 2014).

In this way, hairy roots are very interesting from a biotechnological viewpoint, because of a great quantity of biomass can be obtained in short times since they have fast growth (Agostini et al., 2013). Hairy roots production has the advantage of being independent of climate or to the effect of pathogens, as could occur with plant roots

growing in the field. Recent remediation works have reported the use of hairy roots as tools for the removal of cationic dyes (Govindwar and Kagalkar, 2011; Khandare and Govindwar, 2015; Lokhande et al., 2015; Watharkar et al., 2013). As secretion of root exudates or enzymes around roots zones seem to be efficient systems for the biodegradation of textile dyes, the majority of studies involving hairy roots for dyes removal are mainly focused on the biodegradation capacity of the biological material. However, up to date, studies involving adsorption processes based on the use of hairy roots for the removal of cationic dyes from wastewaters are really scarce. In this way, the aim of our work is to contribute with novel information through the evaluation of the biosorbent potential of hairy roots of tobacco plants for the removal of the cationic dye from aqueous solutions. This work opens the door for new studies in this field. Tobacco can be cultivated under different conditions, generating biomasses with different functional groups. So, tobacco can be used to remove specific contaminants from aqueous media. Depending of the required contaminant, it is possible to modify the cultivation media and provide a good sorbent.

Therefore, the biosorbent was characterized according to the point of zero charge (pH_{ZPC}), Boehm titration method, Fourier transform infrared spectroscopy (FT−IR), scanning electron microscopy (SEM) and energy X−ray dispersive spectroscopy (EDS). A 3^2 full factorial design was used to study the effects of experimental variables on the biosorption. Kinetic studies were developed, and the obtained data were evaluated by the pseudo−first order and pseudo−second order models. Isotherm studies were also carried out, and experimental data were fit by Langmuir, Freundlich, and Sips models. Thermodynamic parameters including standard Gibbs free energy change (ΔG^0), standard enthalpy change (ΔH^0), and standard entropy change (ΔS^0) were estimated. Different reagents were evaluated for desorption of MG

and the reutilization capacity of THR was also studied. THR biosorbent was also tested in a simulated industrial effluent. For the first time, this work demonstrates the potential of THR for adsorptive removal of MG from aqueous solutions.

Materials and methods

Tobacco hairy roots production and preparation

Tobacco (*Nicotiana tabacum*) hairy roots (THR) were grown on Murashige and Skoog (MS) (Murashige and Skoog, 1962) liquid medium at 25 ± 2 ºC in the dark, on an orbital shaker at 70 rpm, as was previously described (Sosa Alderete et al., 2009). They were maintained for successive subcultures each 30-35 d in MS medium. After 35 d of culture, roots were harvested, dried and lyophilized using a LABCONCO equipment (Mod. Freezone 6) until they reached constant weight. Dried roots were used for successive experiments.

Characterization techniques

In order to know the surface charge of the THR at the working pH, the point of zero charge (pH_{ZPC}) was determined through an adaptation of a previously reported procedure (Rivera-Utrilla et al., 2001). Firstly, 50 ml of 0.01 mol L^{-1} NaCl solutions were placed in closed Erlenmeyer flasks. The pH values were adjusted to 2, 4, 6, 8, 10, and 12 by the addition of 0.1 mol L^{-1} NaOH or HCl solutions. Then, 0.15 g of THR was added and the final pH was measured after 48 h of agitation at room temperature. The pH_{ZPC} was the point where the curve of pH_{final} vs. $pH_{initial}$ intersects the line $pH_{initial} = pH_{final}$.

The acidity and basicity of the biosorbent was evaluated by the Boehm titration (Goertzen et al., 2010). The groups with acidic activity present in the THR have

different pK_a values, so they could be determined potentiometrically using basic solutions of different strengths. Taking into account the difference in base volumes spent between consecutive titrations, the different acid groups were quantified and expressed as meqH_3O^+ per gram of biosorbent. An inverse process was performed to determine the total basicity of THR.

Fourier transform infrared spectroscopy (FTIR) (Shimadzu, Prestige 21, Japan) was used for the identification of functional groups present in the biosorbent (Silverstein et al., 2007). Samples were analyzed using potassium bromide (KBr) pellets (~ 0.5 mg of sample with 100 mg KBr and compressing the mixture into a 13−mm diameter pellet).

The morphology of the biosorbent and the main elements present on the THR were evaluated by scanning electron microscopy (SEM) coupled to energy X−ray dispersive spectroscopy (EDS) (Jeol, JSM−6610LV, Japan). Before analysis, samples were coated with a 15−nm−thick Au/Pd layer with a sputter coating system. Both FTIR and SEM analytical techniques were performed before and after the biosorption process in order to identify possible changes on the biosorbent surface.

Reagents and solutions

Malachite green dye (4−{[4−(Dimethylamino)phenyl](phenyl)methylidene} −N,N−dimethylcyclohexa−2,5−dien−1−iminium chloride); C.I. 42000; λ_{max}=619 nm; molecular formula $C_{23}H_{25}ClN_2$; molecular weight 364.91 g mol^{-1}) was obtained from Vetec (Brazil). A stock standard solution of 1000 mg L^{-1} was prepared, and the subsequent dilutions were made with deionized water from this solution. The pH of solutions was adjusted with 0.1 mol L^{-1} NaOH and HCl solutions using a pH meter (Digimed, DM 20, Brazil) for the measurements.

Biosorption experiments

The biosorption experiments were performed in a batch system. Initially, 25 mL of 50 mg L^{-1} MG solutions were prepared in Erlenmeyer flasks. The pH of each solution was adjusted to pH 3, 5, and 7. After, 25, 50, and 75 mg (dry basis) of the biosorbent were placed in the previous solutions. The flasks were stirred at 200 rpm in a thermostatic agitator (Marconi, MA 093, Brazil) for 120 min at room temperature. Finally, the solid phase was separated by centrifugation (Centribio, 80−2B, Brazil) at 3000 rpm for 5 min.

The kinetic experiments were developed under the optimal conditions (above determined). Thus, 25 mL of MG solution, with initial dye concentrations of 50 and 100 mg L^{-1} were tested. The pH was adjusted to 7. Then, 25 mg of THR were added to each solution. Different contact times, from 0 to 120 min, were evaluated (samples were withdrawn at different time intervals), at room temperature and under a stirring rate of 200 rpm.

The isotherm studies were carried out in a thermostatic agitator at 298, 308, 318, and 328 K. Erlenmeyer flasks containing 25 mL of MG solutions with initial concentrations from 25 to 300 mg L^{-1} were prepared, and the pH of each solution was adjusted to 7. The flasks were placed in the thermostatic agitator to attain the adequate temperature. Then, 25 mg of THR were added to each flask, and agitation at 200 rpm was maintained until the equilibrium. Finally, solid phase was separated by centrifugation.

For all experiments, the MG concentrations were determined in the upper aqueous phase by spectrophotometry (Biospectro SP−22, Brazil), at the maximum wavelength. Calibration was performed against aqueous standards and blank solutions. The dye removal percentage (R, %) was calculated by Equation (1). Biosorption

capacity at any time (q_t (mg g^{-1})) and at equilibrium (q_e (mg g^{-1})) were calculated by Equations (2) and (3), respectively (Crini and Badot, 2008).

$$R = \frac{(C_0 - C_e)}{C_0} 100 \quad (1)$$

$$q_t = \frac{V(C_0 - C_t)}{m} \quad (2)$$

$$q_e = \frac{V(C_0 - C_e)}{m} \quad (3)$$

where, C_0 is the initial dye concentration in liquid phase (mg L^{-1}), C_t is the dye concentration in liquid phase at any time (mg L^{-1}), C_e is the equilibrium dye concentration in liquid phase (mg L^{-1}), m is the amount of adsorbent (g) and V is the volume of solution (L).

Experimental design for optimization of variables

Considering that pH and biosorbent concentration are variables that play an important role on biosorption process, the effects of pH (5, 7, and 9) and THR concentration (1, 2, and 3 g L^{-1}) on both, the dye removal and biosorption capacity, were evaluated through a three−level two factor 3^2 full factorial design. The dye removal and the biosorption capacity (q) were represented as a function of independent variables, through the polynomial quadratic equation showed in Equation (4):

$$q = a + \sum_{i=1}^{n} b_i x_i + \sum_{i=1}^{n} b_{ii} x_i^2 + \sum_{i=1}^{n-1} \sum_{j=i+1}^{n} b_{ij} x_i x_j \quad (4)$$

where, "a" is the constant coefficient, "b_i" are the linear coefficients, "b_{ij}" are the interaction coefficients, "b_{ii}" are the quadratic coefficients, "x_i" and "x_j" are the coded values of the variables. The statistical significance of the nonlinear regression was determined by the Student's test, the second order model equation was evaluated by the Fischer's test and the proportion of variance explained by the obtained model was given

by the coefficient of determination, R^2 (Rêgo et al., 2013). Experimental runs were performed at random and the results were analyzed using Statistica version 9.1 (StatSoft Inc., USA) software.

Kinetic, isotherms, and thermodynamic studies

Kinetic, equilibrium, and thermodynamic studies are fundamental to evaluate an alternative biosorbent material (Liu and Liu, 2008). From the kinetic viewpoint, the biosorption of MG on THR was evaluated by the pseudo first−order (Lagergren, 1898), and pseudo second−order (Ho and McKay, 1998) models, which are shown in Equations (5) and (6), respectively.

$$q_t = q_1(1 - \exp(-k_1 t)) \quad (5)$$

$$q_t = \frac{t}{(1/k_2 q_2^{\,2}) + (t/q_2)} \quad (6)$$

where, k_1 and k_2 are the rate constants of pseudo–first order (min^{-1}) and pseudo–second order (g mg^{-1} min^{-1}) models, respectively; q_1 and q_2 are the theoretical values for the biosorption capacity (mg g^{-1}).

Regarding equilibrium, three isotherm models were tested in order to represent the MG biosorption on THR. Langmuir model (Equation (7)) (Langmuir, 1918) assumes that the biosorption sites have the same energy and the biosorption occurs by a monolayer formation; Freundlich model (Equation (8)) (Freundlich, 1906) assumes biosorption in a heterogeneous surface; and Sips model (Equation (9)) (Sips, 1948) contains elements from both Langmuir and Freundlich models.

$$q_e = \frac{q_m k_L C_e}{1 + (k_L C_e)} \quad (7)$$

$$q_e = k_F C_e^{1/nF} \quad (8)$$

$$q_e = \frac{q_{mS}(k_S C_e)^{mS}}{1+(k_S C_e)^{mS}} \quad (9)$$

where, q_m is the maximum biosorption capacity (mg g^{-1}), k_L is the Langmuir constant (L mg^{-1}), k_F is the Freundlich constant ((mg g^{-1})(mg L^{-1})$^{-1/nF}$), $1/n_F$ is the heterogeneity factor, q_{mS} is the maximum biosorption capacity from Sips (mg g^{-1}), k_S is the Sips constant (L mg^{-1}), and m_S is the exponent of the Sips model. Another relevant aspect of the Langmuir model is the equilibrium factor, R_L, which is expressed by the following Equation:

$$R_L = \frac{1}{1+(K_L C_e)} \quad (10)$$

For R_L=1, the isotherm is linear, 0<R_L<1indicates a favorable process and, R_L=0 indicates an irreversible process (Hamdaoui and Naffrechoux, 2007).

From the thermodynamic point of view, the biosorption of MG on THR was evaluated according to the standard values of Gibbs free energy change (ΔG^0, kJ mol^{-1}), enthalpy change (ΔH^0, kJ mol^{-1}) and entropy change (ΔS^0, kJ mol^{-1} K^{-1}), which were estimated by Equations (11−13) (Anastopoulos and Kyzas, 2016; Milonjic, 2007).

$$\Delta G^0 = -RT\ln(\rho K_e) \quad (11)$$

$$\Delta G^0 = \Delta H^0 - \Delta S^0 T \quad (12)$$

$$\ln(\rho K_e) = \frac{\Delta S^0}{R} - \frac{\Delta H^0}{RT} \quad (13)$$

where, K_e is the equilibrium constant (L g^{-1}) (based in the parameters of the best fit isotherm model), T is the temperature (K), R is 8.31x10^{-3} kJ mol^{-1} K^{-1} and ρ is the solution density (g L^{-1}).

Modeling and parameter estimation

The kinetic, equilibrium, and thermodynamic parameters were determined by nonlinear regression using Statistic 9.1 software (Statsoft, USA). The fit quality was checked trough the coefficient of determination (R^2) and average relative error (ARE) (Equations (14) and (15)) (Dotto et al., 2013).

$$R^2 = \left(\frac{\sum_i^n \left(q_{i,exp} - \overline{q}_{i,exp}\right)^2 - \sum_i^n \left(q_{i,exp} - q_{i,model}\right)^2}{\sum_i^n \left(q_{i,exp} - \overline{q}_{i,exp}\right)^2} \right) \quad (14)$$

$$ARE = \frac{100}{n} \sum_{i=1}^{n} \left| \frac{q_{i,\mathrm{model}} - q_{i,\mathrm{exp}}}{q_{i,\mathrm{exp}}} \right| \quad (15)$$

where, $q_{i,model}$ is each value of q predicted by the fitted model, $q_{i,exp}$ is each value of q measured experimentally, $\overline{q}_{i,\mathrm{exp}}$ is the average of q experimentally measured, and n is the number of experimental points. In the isotherms fit, the R^2_{adj} (adjusted determination coefficient) was also used, since the models have different numbers of parameters.

Desorption experiments

Desorption studies were carried out in order to evaluate the possibility to reuse the biosorbent. The following eluents were assayed: NaCl, citric acid, and acetic acid, at concentrations between 0.5 and 2 mol L^{-1}. Thus, a volume of 50 mL of each eluent solution was added to the MG−loaded THR and the resulting mixture was agitated with rotator shaker at 200 rpm for 180 min. Subsequently, samples were centrifuged and MG concentration released in the desorbing solution was also determined by UV–vis spectrophotometry.

Application of THR biosorbent on a simulated industrial effluent

A synthetic effluent was prepared on the basis of effluents from the textile industry at the dyeing stages, as was previously described (Bretanha et al., 2016). The

simulated effluent (pH=7) contained the following substances: NaCl (300 mg L^{-1}), Na_2CO_3 (200 mg L^{-1}), CH_3COONa (200 mg L^{-1}), CH_3COOH (1000 mg L^{-1}), humic acid (50 mg L^{-1}), sodium dodecyl sulfate (50 mg L^{-1}), and cationic dyes including MG (50.0 mg L^{-1}), crystal violet (10 mg L^{-1}), and methylene blue (10 mg L^{-1}). For the experiment, 25 mg of THR biomass was placed into conic flask containing 50.0 mL of the simulated effluents. The mixture was stirred at 200 rpm for 120 min at room temperature. Then, the solid phase was separated by centrifugation at 3000 rpm for 5 min. The treatment efficiency was determined performing a spectrophotometric scanning from 300 to 800 nm, before and after the biosorption.

Results and discussion

Characteristics of THR biomaterial

THR biosorbent was characterized according to the point of zero charge (pH_{zpc}), acidity and basicity, FT−IR, SEM, and EDS. The pH_{zpc} of the biosorbent was 6.80. This shows that at pH values lower than 6.80, the surface of the biosorbent is positively charged, while the surface is negatively charged at pH values higher than 6.80. The values of carboxylic, lactonic, and phenolic groups were 0.25, 0.40, and 3.30 meq g^{-1}, respectively. Consequently, the total acidity on the THR surface was 3.95 meq g^{-1}. The total basicity was 0.50 meq g^{-1}.

The FT−IR spectra of biosorbent before (THR) and after the biosorption process with MG dye are depicted in Figure 1. The THR spectrum (before biosorption) shows the main intense bands around 3400, 2900, 2850, 1650, 1400, 1250, and 1100 cm^{-1}. The broad band centered at 3400 cm^{-1} is mainly due to the O−H and N−H stretching. The stretching of C−H and CH_2 can be visualized at 2900 and 2800 cm^{-1}, respectively. The

band observed at 1650 cm^{-1} is due to the C=O stretching vibration. The C−H deformation can be seen at 1400 cm^{-1}. The C−N and C−O stretching vibration are visualized at 1250 cm^{-1} and 1100 cm−1, respectively. The FT−IR spectrum of THR reveals that there are several functional groups, such as carboxyl and hydroxyl, on the biosorbent surface, that could be able to bind with the textile dye. After biosorption (THR loaded MG), no significant changes were observed in the spectra, which suggest that no chemical links were formed or broken during the biosorption process, indicating that a physical process occurred.

Figure 2 shows the SEM images of THR biosorbent before and after the biosorption of MG. Figure 2(a) shows that THR have an uneven and rough surface, with cavities and protuberances. These textural characteristics are suitable to accommodate the molecules of MG on the surface of the biomass. The surface of the MG dye−loaded biosorbent seen in Figure 2(b) is clearly different from that of the THR before biosorption. Thus, a smoothing in the surface texture of the biosorbent is observed, where cavities and protuberances of the THR disappeared, which indicates that the biosorption of the colored molecules on the biosorbent surface occurred.

The EDS spectra of THR biosorbent before and after biosorption process can be seen in Figure 3. The spectrum of THR (Figure 3(a)) shows emission bands at 0.3 keV due to C, 0.5 keV due to O, 1.0 keV due to Na, 1.3 keV due to Mg, 2.0 keV due to P, 2.3 keV due to S, 2.6 keV due to Cl, and at 3.7 and 4.0 keV due to Ca (which is consistent with Ca K-alpha and K-beta X-rays, which always have these energies). All these elements are in agreement with the biological matrix of THR. After biosorption of MG dye, some elements cannot be observed in the spectrum (Figure 3(b)). For instance, Fe, Na, and K are not present after the biosorption process. It is possible that a fraction of these elements has been leached to the solution during the biosorption.

Experimental design for optimization of MG biosorption

The experimental design matrix and the results obtained from a 3^2 full factorial design are presented in Table I. Analysis of variance (ANOVA) was employed to verify the significance of THR concentration and pH on the responses (dye removal and biosorption capacity). The ANOVA showed that all the linear and quadratic effects and the interaction effects were significant ($p \leq 0.05$). The statistical polynomial quadratic models, which represent the dependence of MG removal percentage (R) and biosorption capacity (q) in relation to the THR concentration (x_1) and pH (x_2), are depicted in Equations (13) and (14), respectively:

$$R = 49.0 + 0.7\,x_1^2 + 5.7\,x_2^2 + 5.0\,x_1 + 37.5\,x_2 - 1.8\,x_1x_2 \quad (13)$$

$$q = 11.2 + 2.8\,x_1^2 + 2.9\,x_2^2 - 6.4\,x_1 + 11.5\,x_2 - 6.6\,x_1x_2 \quad (14)$$

In order to verify the prediction and significance of the models, analysis of variance and Fisher F−test were used. The high values of coefficients of determination (R^2 = 0.98 and 0.96, respectively) showed that the models were significant. The calculated Fisher values (F_{calc} = 188.2 and 48.56) were several times superior to standard Fisher value (F_{std} = 3.10), indicating that the models were predictive.

Then, the statistical models were used to generate the response surfaces (Figure 4), which represents R and q as a function of independent variables. Figure 4(a) shows that the highest MG removal percentage (R) is reached at pH 7. As the removal of MG was only due to a biosorption process, this behavior can be explained since at this pH, the surface of the biosorbent is negatively charged, so possible electrostatic interactions can occur with the MG cationic dye (positively charged). On the other hand, an increase of THR biomass did not cause a significant variation of dye removal (Figure 4(a)). Finally, Figure 4(b) shows that q response increases with the decrease of THR concentration, and when pH values increase. Based on the statistical optimization

results, it was concluded that the optimal conditions to obtain higher R and q values were pH 7 and biosorbent concentration of 1 g L^{-1}. Under these conditions, the dye removal percentage was around 92% and the biosorption capacity was 44.3 mg g^{-1}.

Kinetic experiments and modeling

The biosorption kinetic curves of MG on THR biomass can be seen in Figure 5. It is important to highlight that after 10 min, a marked increase in q_t was observed; and then, this increase was less than the previous one. The equilibrium was attained around 120 min.

In order to find an appropriate model that represents the experimental results, pseudo−first (PFO) and pseudo−second order (PSO) models were fitted to the experimental data. The kinetic parameters are presented in Table II. The selection of the most adequate model was based according to the coefficient of determination (R^2), and the average relative error (*ARE*). The highest R^2 and the lowest *ARE* values were found using the PSO model. It can be observed that the q_2 values increased from 50 to 100 mg L^{-1}, which confirms that the biosorption capacity is higher at higher MG concentration. The h_0 (initial biosorption rate) values also increased with the initial concentration of MG, indicating that at the initial stages, the biosorption was faster when an initial concentration of 100 mg L^{-1} was used. On the other hand, it is important to mention the q_2 values are similar to those obtained experimentally (q_{exp}), which confirms the predictive potential of the model for values of biosorption capacity obtained in the laboratory.

Equilibrium and thermodynamic results

The isotherms of MG dye onto THR biomass were shown in Figure 6. Four different temperatures were assayed: 298, 308, 318, and 328 K. It can be observed an initial increase in the biosorption capacity (suggesting a great affinity between MG dye and the variety of functional groups of THR), tending a convex shape, which is associated with monolayer biosorption (Blázquez et al., 2010). In this figure, it can be also seen that an increase of temperature provokes an increase of biosorption capacity. This behavior is directly related with an endothermic biosorption process, which is favored at high temperatures. The thermodynamic study will confirm the nature of the biosorption through the positive value of enthalpy change obtained (please, see later).

With the aim to find the most suitable correlation for the equilibrium curves and to estimate the isotherm parameters, three models (Langmuir, Freundlich, and Sips) were fitted to the experimental data. Table III shows the isotherm parameters of MG biosorption at all studied temperatures. The experimental data were not in concordance with Freundlich equilibrium model. Although both Langmuir and Sips isotherm models adequately describe the biosorption of MG on THR, the highest R^2 and R^2_{adj} and the lowest *ARE* values were obtained by using the Sips model. Therefore, it was selected as the most adequate to represent the equilibrium biosorption.

The maximum biosorption capacity (q_{ms}) reached a value of 277.2 mg g^{-1} at 328 K. This value is better than several equilibrium biosorption values reported in the literature based on the use of other materials involving MG biosorption studies (Aksakal et al., 2009; Lim et al., 2016; Mohammad et al., 2017). This indicates that THR is a promising biosorbent in terms of biosorption capacity.

Table IV shows the thermodynamic parameters for MG biosorption by using THR biomass. The R^2 value of the linear fit was 0.9833. It can be observed that the values of ΔG^0 were negative, indicating that the biosorption was favorable and

spontaneous at all studied temperatures. The value of enthalpy changes (ΔH^0) was positive, showing that the biosorption was endothermic. Moreover, the magnitude of ΔH^0 suggested that physical interactions were involved in the biosorption process (Mahmoud et al., 2012). Finally, the value of entropy changes (ΔS^0) was positive, indicating that randomness increases at the solid–solution interface during the biosorption process. This thermodynamic behavior has been also obtained by other authors (El Messaoudi et al., 2017; Jia et al., 2017).

Desorption studies

Figure 7 shows the results of the evaluation of different chemical agents (at different concentrations) for desorption of MG from THR biosorbent. It can be seen that the desorption percentage was higher at higher concentrations of NaCl, citric acid, and acetic acid. However, the best results were obtained by using a 2 mol L^{-1} citric acid solution, with a desorption percentage of around 90%. These results are in good agreement with previous contributions and suggest that dye biosorption on THR is mainly governed by electrostatic interactions (Bretanha et al., 2016; Pavan et al., 2014). Regarding the reutilization of the biosorbent, three cycles could be made with good results, although the removal percentage decreased as the number of cycles increased (82.0 and 76.9% of MG removal in the second and the third cycle, respectively).

Comparison with adsorbents reported in the literature for MG adsorption

A comparative study of some adsorption parameters allows us to show the strengths of the THR biosorbent with respect to other ones used and reported previously (Table 5). THR biosorbent shows a maximum adsorption capacity (q_m) that is better than that reported for other biosorbents used for adsorption of the same cationic dye

(Dan et al., 2009; Jerold and Sivasubramanian, 2016; Chen et al. 2014; Santhi et al., 2011; Arellano-Cárdenas et al., 2013). Table 5 also shows two works that have employed higher concentrations of adsorbent for the adsorption of MG, at concentrations similar that those used in this work (Dan et al., 2009; Chen et al. 2014). Clearly, the low biosorbent concentration needed for biosorption of the MG dye turned this sorption process into a more economical alternative, because the consumption of reagents is considerably reduced.

Application of THR for MG biosorption from simulated effluents

In order to verify the applicability of THR biosorbent for removal of MG in a more complex matrix that simulates the biosorption in real conditions, a textile synthetic effluent was assayed. The removal efficiency in the synthetic sample was 87.0 ± 2.3%. Taking into account the complexity of the matrix solution, and the potential interference effects that some compounds could cause on the MG biosorption efficiency, the results obtained are satisfactory and open the possibility to apply the THR biomass for removal of the hazardous cationic dye in real textile effluents.

Conclusions

Tobacco hairy roots were studied for the removal of MG from aqueous solutions. Under optimal conditions, dye removal efficiency was 92%. Regarding kinetic studies, the pseudo−second order model was the most suitable to describe the experimental data of the biosorption. The Sips isotherm model represented suitably the biosorption of MG onto THR, being the maximum biosorption capacity of 277.2 mg g^{-1}. According to thermodynamic evaluation, it was proved that the biosorption was an

endothermic, favorable, and spontaneous process at all the studied temperatures. The biosorbent can be regenerated using 2.0 mol L^{-1} citric acid as eluent agent. THR was useful to remove the cationic dye from simulated textile effluents, reaching a removal percentage of around 87%. THR is a promising and alternative material to treat colored effluents.

Acknowledgments

The authors would like to thank National Council for Scientific and Technological Development (CNPq), Consejo Nacional de Investigaciones Científicas y Técnicas (CONICET), Agencia Nacional de Promoción Científica y Tecnológica (FONCYT) (Project PICT−2015−1338), and Universidad Nacional de Cuyo for the financial support.

References

Agostini, E., Talano, M. A., González, P. S., Oller, A. L. W., and Medina, M. I. (2013) Application of hairy roots for phytoremediation: What makes them an interesting tool for this purpose?, Appl. Microbiol. Biotechnol. 97, 1017-1030.

Aksakal, Ö., Ucun, H., and Kaya, Y. (2009) Application of *Eriobotrya japonica* (Thunb.) Lindley (Loquat) seed biomass as a new biosorbent for the removal of malachite green from aqueous solution, Water Sci. Technol. 59, 1631-1639.

Anastopoulos, I., and Kyzas, G. (2016) Are the thermodynamic parameters correctly estimated in liquid−phase adsorption phenomena?, J. Mol. Liq. 218, 174-185.

Arrellano-Cárdenas, S., López-Cortez, S., Cornejo-Mazón, M., Mares-Gutiérrez, J. (2013) Study of malachite green adsorption by organically modified clay using a batch method, Appl. Surf. Sci. 280, 74-78

Banerjee, S., Sharma, G. C., Gautam, R. K., Chattopadhyaya, M. C., Upadhyay, S. N., and Sharma, Y. C. (2016) Removal of Malachite Green, a hazardous dye from aqueous solutions using *Avena sativa* (oat) hull as a potential adsorbent, J. Mol. Liq. 213, 162-172.

Bañuelos, J. A., García-Rodríguez, O., El-Ghenymy, A., Rodríguez-Valadez, F. J., Godínez, L. A., and Brillas, E. (2016) Advanced oxidation treatment of malachite green dye using a low cost carbon-felt air-diffusion cathode, J. Environ. Chem. Eng. 4, 2066-2075.

Blázquez, G., Calero, M., Hernáinz, F., Tenorio, G., and Martín-Lara, M. A. (2010) Equilibrium biosorption of lead(II) from aqueous solutions by solid waste from olive-oil production, Chem. Eng. J. 160, 615-622.

Bretanha, M. S., Rochefort, M. C., Dotto, G. L., Lima, E. C., Dias, S. L. P., and Pavan, F. A. (2016) *Punica granatum* husk (PGH), a powdered biowaste material for the adsorption of methylene blue dye from aqueous solution, Desalin. Water Treat. 57, 3194-3204.

Chen, Z., Deng, H., Chen, C., Yang, Y., and Xu, H. (2014) Biosorption of malachite green from aqueous solutions by *Pleurotus ostreatus* using Taguchi method, J. Environ. Health Sci. Eng. 12, 63-73

Crini, G., and Badot, P. M. (2008) Application of chitosan, a natural aminopolysaccharide, for dye removal from aqueous solutions by adsorption processes using batch studies: A review of recent literature, Prog. Polym. Sci. 33, 399-447.

Daneshvar, N., Ayazloo, M., Khataee, A. R., and Pourhassan, M. (2007) Biological decolorization of dye solution containing Malachite Green by microalgae *Cosmarium sp*, Bioresour. Technol. 98, 1176-1182.

Das, A. K., Saha, S., Pal, A., and Maji, S. K. (2009) Surfactant-modified alumina: An efficient adsorbent for malachite green removal from water environment, J. Environ. Sci. Health A 44, 896-905.

Dotto, G., Gonçalves, J., Cadaval, T., and Pinto, L. (2013) Biosorption of phenol onto bionanoparticles from *Spirulina sp.* LEB 18, J. Colloid Interface Sci. 407, 450−456.

El Messaoudi, N., El Khomri, M., Dbik, A., Bentahar, S., and Lacherai, A. (2017) Selective and competitive removal of dyes from binary and ternary systems in aqueous solutions by pretreated jujube shell (*Zizyphus lotus*), J. Dispers. Sci. Technol. 38, 1168-1174.

Fomina, M., and Gadd, G. M. (2014) Biosorption: Current perspectives on concept, definition and application, Bioresour. Technol. 160, 3-14.

Freundlich, H. (1906) Over the adsorption in solution, Z. Phys. Chem. 57, 358-471.

Goertzen, S. L., Thériault, K. D., Oickle, A. M., Tarasuk, A. C., and Andreas, H. A. (2010) Standardization of the Boehm titration, Carbon 48, 1252-1261.

Govindwar, S. P., and Kagalkar, A. N. (2011) Phytoremediation technologies for the removal of textile dyes - an overview and future prospects, In *Handbook of Phytoremediation*, pp 472-494, Nova Science Publishers, Inc.

Hamdaoui, O., and Naffrechoux, E. (2007) Modeling of adsorption isotherms of phenol and chlorophenols onto granular activated carbon Part I: Two-parameter models and equations allowing determination of thermodynamic parameters., J. Hazard. Mat. 147, 381-394.

Ho, Y., and McKay, G. (1998) Kinetic models for the sorption of dye from aqueous solution by wood, Proc. Safety Environ. Protect. 76, 183-191.

Jerold, M., and Sivasubramanian, V. (2016) Biosorption of malachite green from aqueous solution using brown marine macro algae *Sargassum swartzii*, Desalin. Water Treat. 57, 25288-25300.

Jha, P., Jobby, R., and Desai, N. S. (2016) Remediation of textile azo dye acid red 114 by hairy roots of Ipomoea carnea Jacq. and assessment of degraded dye toxicity with human keratinocyte cell line, J. Hazard. Mat. 311, 158-167.

Jia, Z., Li, Z., Ni, T., and Li, S. (2017) Adsorption of low-cost absorption materials based on biomass (*Cortaderia selloana* flower spikes) for dye removal: Kinetics, isotherms and thermodynamic studies, J. Mol. Liq. 229, 285-292.

Khandare, R. V., and Govindwar, S. P. (2015) Phytoremediation of textile dyes and effluents: Current scenario and future prospects, Biotechnol. Adv. 33, 1697-1714.

Lagergren, S. (1898) About the theory of so–called adsorption of soluble substances, Kung. Svenska. Vetenskap. 24, 1-39.

Langmuir, I. (1918) The adsorption of gases on plane surfaces of glass, mica and platinum, J. Amer. Chem. Soc. 40, 1361-1403.

Li, L., Peng, A.-h., Lin, Z.-z., Zhong, H.-p., Chen, X.-m., and Huang, Z.-y. (2017) Biomimetic ELISA detection of malachite green based on molecularly imprinted polymer film, Food Chem. 229, 403-408.

Lim, L. B. L., Priyantha, N., and Mohd Mansor, N. H. (2016) Utilizing *Artocarpus altilis* (breadfruit) skin for the removal of malachite green: isotherm, kinetics, regeneration, and column studies, Desalin. Water Treat. 57, 16601-16610.

Liu, Y., and Liu, Y. J. (2008) Biosorption isotherms, kinetics and thermodynamics, Sep. Purif. Technol. 61, 229-242.

Lokhande, V. H., Kudale, S., Nikalje, G., Desai, N., and Suprasanna, P. (2015) Hairy root induction and phytoremediation of textile dye, Reactive green 19A-HE4BD, in a halophyte, *Sesuvium portulacastrum* (L.) L, Biotechnol. Rep. 8, 56-63.

Mahmoud, M. E., Abdel-Fattah, T. M., Osman, M. M., and Ahmed, S. B. (2012) Chemically and biologically modified activated carbon sorbents for the removal of lead ions from aqueous media, J. Environ. Sci. Heal. A 47, 130-141.

Man, L. W., Kumar, P., Teng, T. T., and Wasewar, K. L. (2012) Design of experiments for Malachite Green dye removal from wastewater using thermolysis - coagulation-flocculation, Desalin. Water Treat. 40, 260-271.

Milonjic, S. (2007) A consideration of the correct calculation of thermodynamic parameters of adsorption, J. Serb. Chem. Soc. 72, 1363-1367.

Mohammad, R., Rajoo, A. T., and Mohamad, M. (2017) Coconut fronds as adsorbent in the removal of malachite green dye, J. Eng. Appl. Sci. 12, 996-1001.

Murashige, T., and Skoog, F. (1962) A revised medium for rapid growth and bioassays with tobacco tissue cultures, Plant Physiol. 15, 473-479.

Pavan, F. A., Camacho, E. S., Lima, E. C., Dotto, G. L., Branco, V. T. A., and Dias, S. L. P. (2014) Formosa papaya seed powder (FPSP): Preparation, characterization and application as an alternative adsorbent for the removal of crystal violet from aqueous phase, J. Environ. Chem. Eng. 2, 230-238.

Rêgo, T. V., Cadaval, T. R. S., Dotto, G. L., and Pinto, L. A. A. (2013) Statistical optimization, interaction analysis and desorption studies for the azo dyes adsorption onto chitosan films, J. Colloid Interface Sci. 411, 27-33.

Rivera-Utrilla, J., Bautista-Toledo, I., Ferro-Garca, M. A., and Moreno-Castilla, C. (2001) Activated carbon surface modifications by adsorption of bacteria and

their effect on aqueous lead adsorption, J. Chem. Technol. Biotechnol. 76, 1209-1215.

Santhi, T., Manonmani, S., Vasatha, V., Chang, Y. (2011) A new alternative adsorbent for the removal of cationic dues from aqueous solutions, Arab. J. Chem. 9, 466-474.

Sasidharan Pillai, I. M., and Gupta, A. K. (2016) Electrochemical degradation of malachite green: Multivariate optimization, pathway identification and toxicity analysis, J. Environ. Sci. Health A 51, 1091-1099.

Silverstein, R., Webster, F., and Kiemle, D. (2007) *Spectrometric Identification of Organic Compounds*, John Wiley & Sons, New York, USA.

Sips, R. (1948) On the structure of a catalyst surface, J. Chem. Phys. 16, 490-495.

Sosa Alderete, L., Talano, M., Ibañez, S., Purro, S., Agostini, E., and Medina, M. I. (2009) Establishment of transgenic tobacco hairy roots expressing basic peroxidases and its application for phenol removal, J. Biotechnol. 139, 273-279.

Telke, A. A., Kagalkar, A. N., Jagtap, U. B., Desai, N. S., Bapat, V. A., and Govindwar, S. P. (2011) Biochemical characterization of laccase from hairy root culture of *Brassica juncea* L. and role of redox mediators to enhance its potential for the decolorization of textile dyes, Planta 234, 1137-1149.

Watharkar, A. D., Khandare, R. V., Kamble, A. A., Mulla, A. Y., Govindwar, S. P., and Jadhav, J. P. (2013) Phytoremediation potential of *Petunia grandiflora Juss.*, an ornamental plant to degrade a disperse, disulfonated triphenylmethane textile dye Brilliant Blue G, Environ. Sci. Pollut. Res. 20, 939-949.

Zhang, J., Li, Y., Zhang, C., and Jing, Y. (2008) Adsorption of malachite green from aqueous solution onto carbon prepared from *Arundo donax* root, J. Hazard. Mat. 150, 774-782.

Figure captions

Fig. 1 FTIR spectra of THR before (black line) and after MG (red line) biosorption.

Fig. 2 SEM images of THR before (a) and after MG (b) biosorption.

Fig. 3 EDS spectra of THR biosorbent before (a) and after the biosorption process for MG (b).

Fig. 4 Response surfaces of MG removal (a) and biosorption capacity (b) by THR biosorbent.

Fig. 5 Kinetic adsorption curves of MG in the optimal conditions.

Fig. 6 Experimental adsorption equilibrium curves and Sips isotherm model of MG onto THR biosorbent. Temperatures: 298 K (■), 308 K (■), 318 K (■), and 328 K (■).

Fig. 7 Malachite green desorption by using different eluents.

Table captions

Table 1 Experimental design matrix and results for MG biosorption by tobacco hairy roots.

Table 2 Kinetic parameters for MG biosorption by tobacco hairy roots.

Table 3 Isotherm parameters for MG biosorption by tobacco hairy roots

Table 4 Thermodynamic parameters for MG biosorption by tobacco hairy roots.

Table 5 Comparison of different adsorbents for the biosorption of MG dye.

Fig. 1

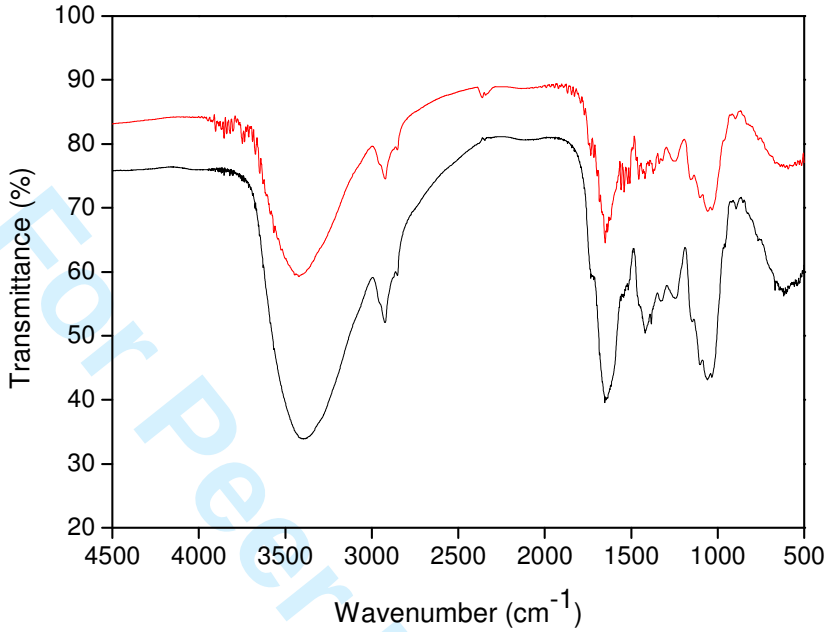

Fig. 2

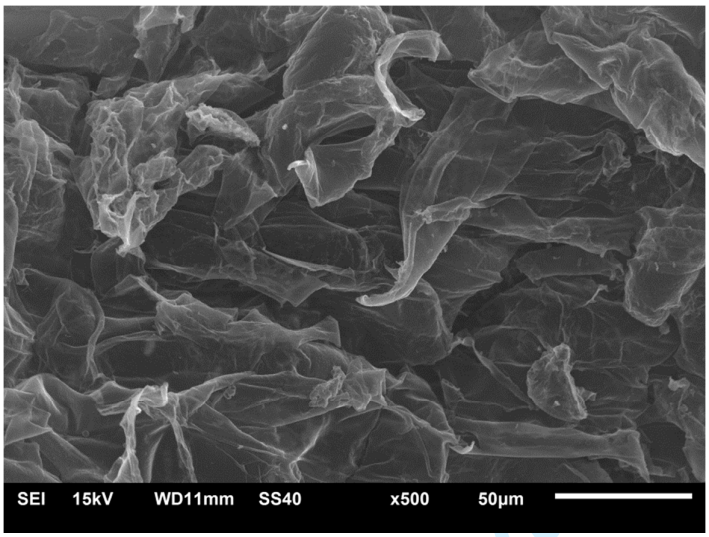

a)

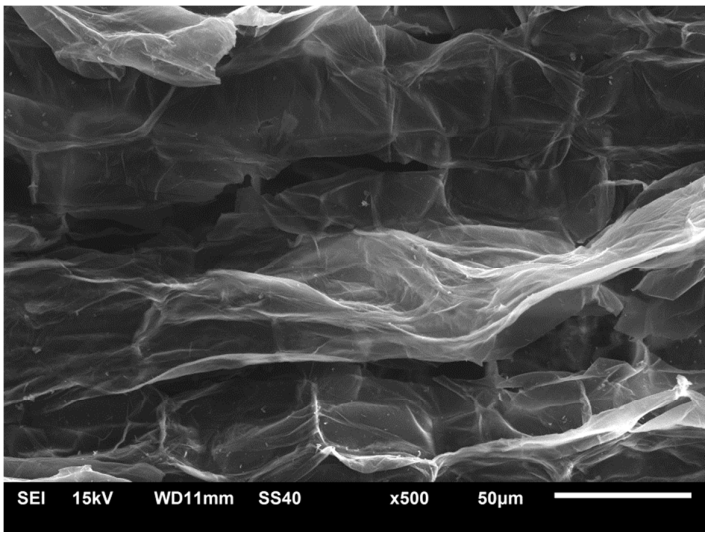

b)

Fig. 3

a)

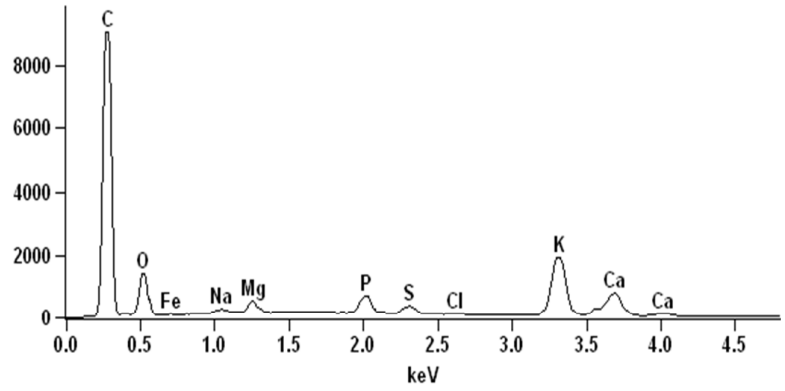
C
O
Fe
Na
Mg
P
S
Cl
K
Ca
Ca
8000
6000
4000
2000
0
0.0
0.5
1.0
1.5
2.0
2.5
3.0
3.5
4.0
4.5
keV

b)

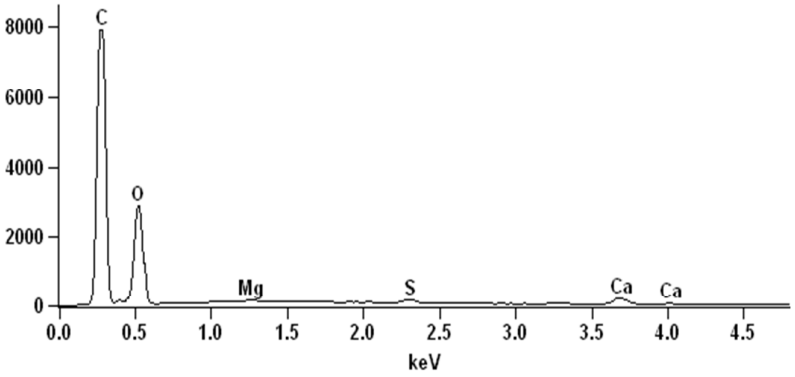
C
O
Mg
S
Ca
Ca
8000
6000
4000
2000
0
0.0
0.5
1.0
1.5
2.0
2.5
3.0
3.5
4.0
4.5
keV

Fig. 4

a)

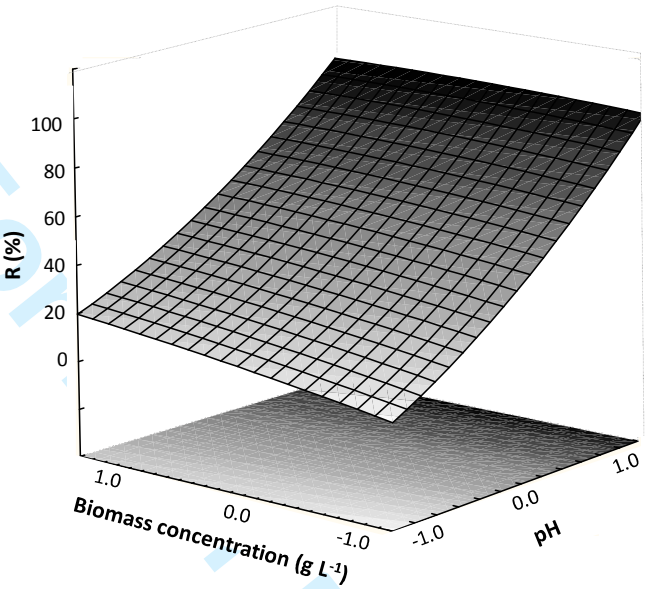
R (%)
100
80
60
40
20
0
1.0
0.0
-1.0
Biomass concentration (g L-1)
-1.0
0.0
1.0
pH

b)

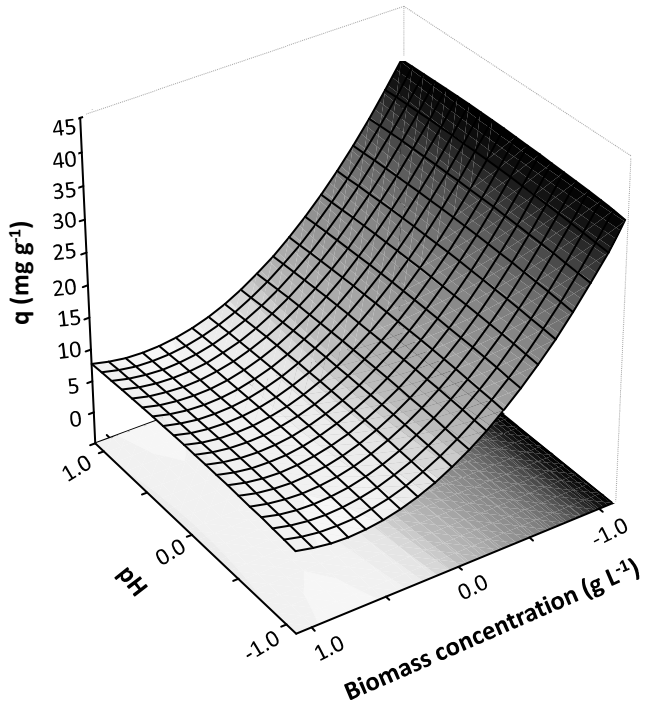
q (mg g-1)
45
40
35
30
25
20
15
10
5
0
1.0
0.0
-1.0
pH
1.0
0.0
-1.0
Biomass concentration (g L-1)

Fig. 5

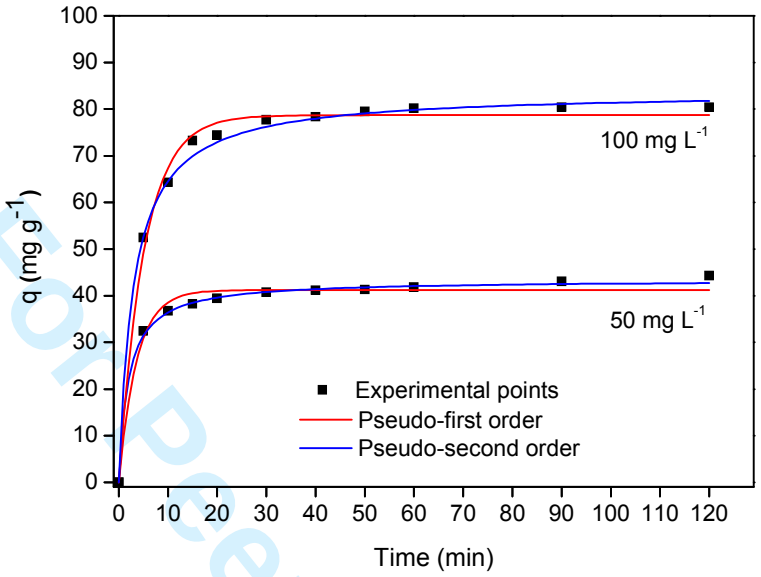

Fig. 6

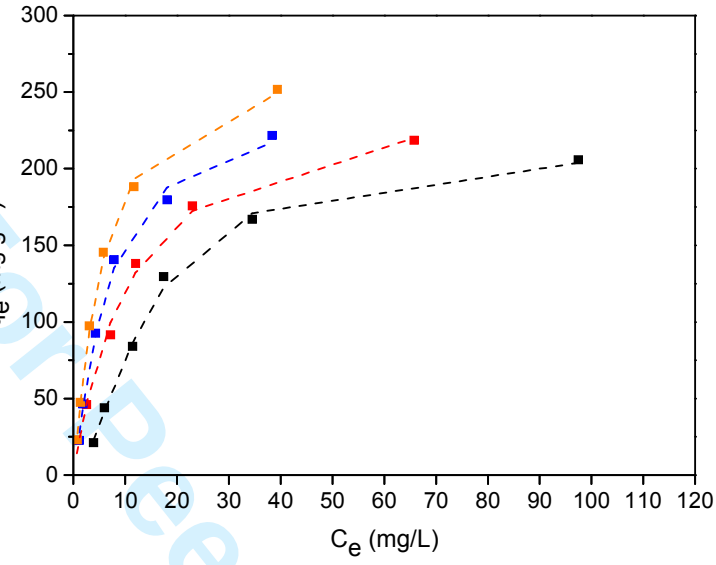

Fig. 7

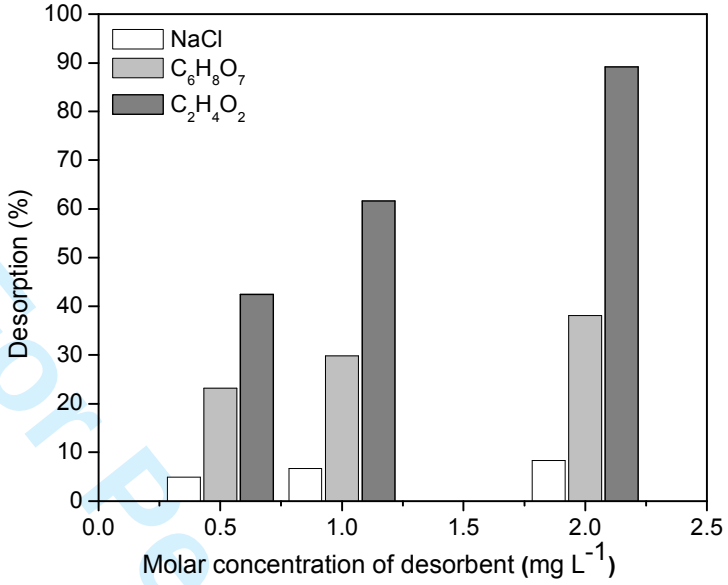

Table 1
Experimental design matrix and results for MG biosorption on tobacco hairy roots.

Experiment	pH [coded form]	THR concentration (g L^{-1}) [coded form]	R (%)*	q (mg g^{-1})*
1	3 [−1]	1 [−1]	13.0 ± 1.7	6.5 ± 1.4
2	3 [−1]	2 [0]	16.3 ± 1.9	4.0 ± 1.3
3	3 [−1]	3 [+1]	20.7 ± 2.1	3.1 ± 1.3
4	5 [0]	1 [−1]	36.4 ± 2.3	16.3 ± 1.6
5	5 [0]	2 [0]	51.6 ± 2.5	13.1 ± 1.5
6	5 [0]	3 [+1]	57.7 ± 2.3	9.5 ± 1.5
7	7 [+1]	1 [−1]	92.5 ± 2.9	44.3 ± 2.6
8	7 [+1]	2 [0]	90.5 ± 2.7	21.9 ± 2.0
9	7 [+1]	3 [+1]	92.5 ± 2.8	14.9 ± 1.3

Note: R: MG removal percentage; q: biosorption capacity.

*Mean ± standard error (n =3).

Table 2
Kinetic parameters for MG biosorption by tobacco hairy roots.

Model	MG	
	50 mg L^{-1}	**100 mg L^{-1}**
Pseudo−first order		
k_1 (min^{-1})	0.275	0.194
q_1 (mg g^{-1})	41.2	78.7
R^2	0.982	0.992
ARE (%)	3.14	2.30
Pseudo−second order		
k_2 (g mg^{-1} min^{-1})	0.012	0.004
q_2 (mg g^{-1})	43.4	83.8
h_0 (mg g^{-1} min^{-1})	22.6	25.4
R^2	0.997	0.997
ARE (%)	1.14	1.22
q_{exp} (mg g^{-1})	44.3	80.4

Table 3
Isotherm parameters for MG biosorption by tobacco hairy roots.

Model	Temperature (K)			
	298	**308**	**318**	**328**
Langmuir				
q_m (mg g^{-1})	263.0	258.6	268.9	293.5
k_L (L mg^{-1})	0.043	0.087	0.121	0.156
R_L	0.071	0.036	0.026	0.020
R^2	0.977	0.995	0.994	0.997
R^2_{adj}	0.972	0.994	0.992	0.996
ARE (%)	18.62	7.86	8.93	7.69
Freundlich				
k_F ((mg g^{-1}) (mg L^{-1})$^{-1/nF}$)	28.2	44.2	45.7	59.6
$1/n_F$	2.217	2.518	2.226	2.449
R^2	0.913	0.959	0.955	0.945
R^2_{adj}	0.895	0.950	0.946	0.934
ARE (%)	83.67	20.60	26.00	30.97
Sips				
q_{ms} (mg g^{-1})	213.4	259.1	244.1	277.2
k_S (L mg^{-1})	0.069	0.087	0.153	0.180
mS	1.607	0.995	1.184	1.123
R^2	0.997	0.995	0.996	0.998
R^2_{adj}	0.995	0.992	0.994	0.997
ARE (%)	3.71	7.85	5.37	4.06

Table 4
Thermodynamic parameters for MG biosorption by tobacco hairy roots.

T (K)	ΔG^0 (kJ mol^{-1})*	ΔH^0 (kJ mol^{-1})*	ΔS^0 (kJ mol^{-1} K^{-1})*
298 K	−24.1±0.2	29.7±0,7	0.18±0.02
308 K	−25.6±0.1		
318 K	−27.8±0.1		
328 K	−29.4±0.1		

*Mean ± standard error(n = 3).

Table 5
Comparison of different adsorbents for the biosorption of MG dye.

Biosorbent	q_m (mg g^{-1})	pH	[Biosorbent] (g L^{-1})	Reference
Surfactant-modified alumina	185	5.3	10.0	Das et al., 2009
S. swartzii macroalga	111	10.0	0.5	Jerold et al., 2016
P. ostreatus macrofungus	125	7.0	4.0	Chen et al., 2014
A. squmosa seed	25.9	6.0	4.0	Santhi et al., 2011
Organically modified clay	56.0	3.0	8.0	Arellano-Cárdenas et al., 2013
THR	277	7.0	1.0	This work